PCCP

Accepted Manuscript

ROYAL SOCIETY OF CHEMISTRY

www.rsc.org/pccp

METHYL ROTORS IN FLAVOPROTEINS

Jesús I. Martínez,*[,a] Pablo J. Alonso,[a] Inés García-Rubio[b,c] and Milagros Medina[d]

[a]Instituto de Ciencia de Materiales de Aragón, Universidad de Zaragoza-Consejo Superior de Investigaciones Científicas, Facultad de Ciencias, C/Pedro Cerbuna 12, 50009 Zaragoza, Spain

[b]Laboratory of Physical Chemistry, ETH Zurich, Vladimir-Prelog-Weg 2, 8093 Zürich, Switzerland

[c]Centro Universitario de la Defensa, Ctra de Huesca s/n, 50090 Zaragoza, Spain

[d]Departamento de Bioquímica y Biología Molecular y Celular and Instituto de Biocomputación y Física de Sistemas Complejos (BIFI), Universidad de Zaragoza, C/Pedro Cerbuna 12, 50009 Zaragoza, Spain

ABSTRACT

In this contribution we present the study of the thermal dependence of the ENDOR spectra of Flavodoxin at low temperatures which reveals the dynamics of the methyl groups bound to the flavin moiety in flavoproteins. The methyl groups behave as quantum rotors locked by a deep rotational well and undergoing a tunneling process. At room temperature, methyl rotors are still locked and the hopping motion is slow. This picture of the dynamics of the methyl groups of the flavin ring is quite different to the one usually accepted and has relevant consequences on the understanding of the mechanisms of flavoproteins.

1.- INTRODUCTION

Flavoproteins are a large family of proteins that use flavin mononucleotide (FMN) or flavin adenine dinucleotide (FAD) as cofactors in all type of organisms.[1] In most of them these cofactors act as redox centers involved in a large variety of metabolic processes where electron and/or hydride transfer takes place, including: aerobic and anaerobic metabolisms, cell respiration, photosynthesis, denitrification, DNA photoreparation, light sensing, light emission, synthesis of natural products, elimination of reactive oxygen species or apoptosis.[2] Because of this versatility in functions, flavin derivatives are also promising precursors for functional materials.

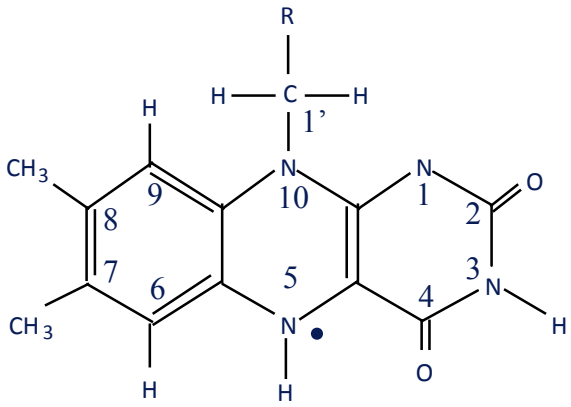

Figure 1.- Molecular structure of the flavin isoalloxazine ring in the neutral semiquinone state. Relevant atomic positions are labelled. For flavin mononucleotide (FMN), the cofactor of WT Fld, the radical, R, bound to C1' consists in a ribityl chain followed by a phosphate group. For Lumiflavin, R = H, a methyl group binds to N10.

The ability of flavin cofactors to mediate in these biochemical processes is related to their unique redox properties. Their flavin moiety can be found in three oxidation states; fully oxidized (ox), semiquinone (one-electron partially reduced, sq) and hydroquinone (two-electrons fully reduced, hq). Despite the semiquinone state of free flavins is not stable in solution, the interaction of the flavin ring with the protein environment highly modulates its midpoint reduction potentials for the ox/sq and sq/hq transitions and makes the semiquinone state stable in many flavoproteins and flavoenzymes. This gives them the possibility to mediate electron transfer processes involving donor/acceptors only able to exchange one electron at a time with those that

obligatory need to exchange two simultaneously (as dehydrogenation or hydride transfer steps involving pyridine nucleotides).[3-6]

Therefore, the understanding of how the structure of the flavin and its interaction with the nearest protein environment modulate the chemical behavior within the protein environment is of great interest. Different studies have already analyzed how the flavin-protein and flavin-substrate interactions control the oxido-reduction and electronic properties, as well as the reactions consequence of them in different flavoproteins.[3,5,7-14] Additionally, the study of the electronic structure, that is, the morphology and properties of the relevant electronic orbitals involved in those electron-transfer processes, is also a field of interest to fulfill the understanding of these systems. Due to the fact that the semiquinone state of the flavin has an unpaired electron, electron paramagnetic resonance (EPR) related methods are especially suitable for the study of its electronic structure. In this state, the unpaired electron occupies an extended π orbital, and EPR techniques allow detecting its electron spin and mapping the orbital through hyperfine couplings with nuclear spins in the flavin ring. Thus, data from ESEEM, ENDOR and quantum chemical calculations have determined specific properties of the semioccupied orbital of the flavin semiquinone within the flavoprotein, and specifically those related with positions that have been notice as relevant for electrons exchanging in and out of the flavin; namely C6, C8 and N5 (for atom labelling, see Figure 1).[6,15-18] In many of those studies *Anabaena* flavodoxin (Fld) was used as model flavoprotein, since it is able to stabilize nearly 100% of its semiquinone state.[6,19-22] In a previous study[23] we used ESEEM experiments to show that the combination of several EPR related techniques yields a detailed map of the flavin electronic structure. At that moment, differences between the hyperfine constants obtained from ENDOR and ESEEM experiments were attributed to the different experimental temperatures. A temperature-dependent process was therefore predicted.

In order to determine the existence and nature of this process, a systematic ENDOR study of Fld semiquinone as a function of the temperature has been undertaken. The study has been carried out in two different Fld samples: WT-Fld (FMN containing) and apoFld reconstituted with lumiflavin (hereafter Lumi-Fld), where the ribityl chain and the phosphate of FMN at position 10 is replaced by a methyl group (see Figure 1). Our results are discussed on the basis of a dynamic process of the methyl group bound to the C8 position of the flavin ring.

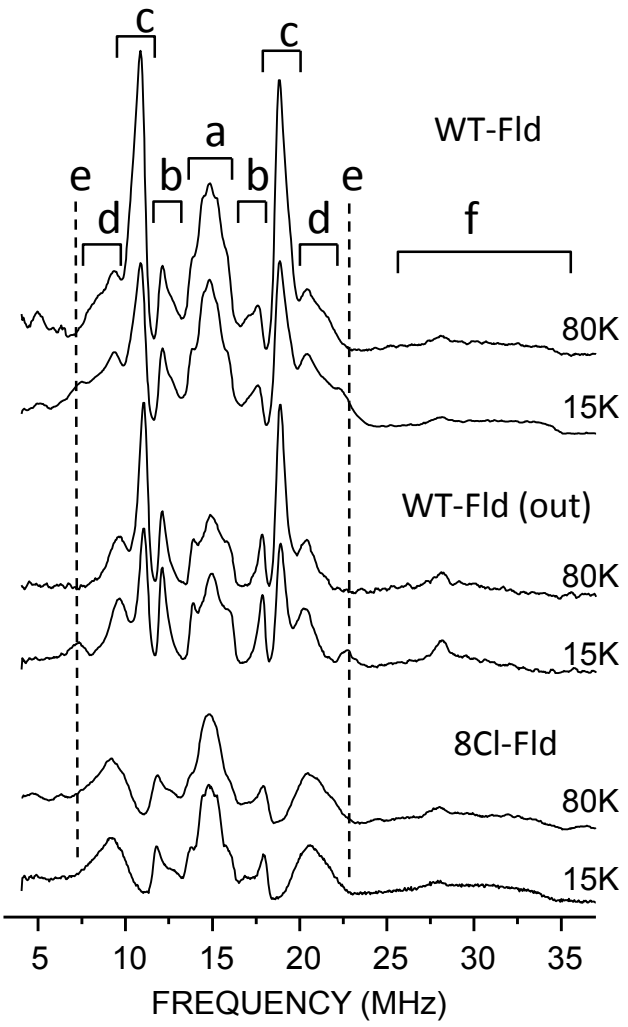

a.- "Matrix" protons; b.- H6; c.- $CH_3(8)^A$;
d.- H^sC1'; e.- $CH_3(8)^{E+}$; f.- H5

Figure 2.- Pulse ENDOR spectra of WT-Fld and 8Cl-Fld measured at two different temperatures, 15 K and 80 K. Spectral features have been assigned to specific proton hyperfine couplings and labelled. Signals a, b, c, d and f, have been assigned on the basis of previously reported ENDOR measurements on several flavoproteins. In WT-Fld spectra (top), signal d seems to span larger at lower temperatures. Measurements in a magnetic field position 2 mT out of the position of the CW-EPR resonance maximum (centre) show in this frequency region two signals (d and e) properly resolved. As signal e disappears in spectra of 8Cl-Fld (bottom) it can be assigned to $CH_3(8)$. Note that signal c also disappears for this sample.

2.- RESULTS AND DISCUSSION

2.1.- EXPERIMENTAL RESULTS

To characterize the postulated temperature activated process,[23] proton ENDOR experiments with systematic variation of the temperature between 15 K and 80 K were carried out.

The spectra of WT-Fld at 15 and 80 K are shown in Figure 2 (top spectra). All the detected spectral features correspond to protons within the flavin ring in the weak-coupling regime, which are easy to assign from previously reported measurements.[25,26] The region containing the matrix peak and very weakly interacting protons (solvent and protein protons together with H3, CH_3(7) and H9 of the flavin ring) is marked with the label a in Figure 2. Signals assigned to flavin proton H6, labelled as b, CH_3(8), labelled as c, and H5, labelled as f, yield hyperfine constants (see Table 1) fully coherent with those previously reported for the same protein.[23] Positions of these lines do not change at the two depicted temperatures, but it is evident that signals assigned to the methyl protons CH_3(8) gain relative height at 80 K.

On the other hand, the shape of the features labelled as d in Figure 2 (top spectra), and occupying the (7 MHz-10 MHz) and (20 MHz-23 MHz) regions of the spectra are different at 15 K and 80 K, spanning largely at 15 K. Features at these regions have been previously assigned to one of the two protons of C1', the one most strongly coupled, H^sC1'.[23,25,26] Taking this assignment, the broader signal at 15 K would indicate a larger anisotropy of the hyperfine coupling of this proton that should be understood on the basis of a temperature dependent process. Although dynamics or thermal configuration changes of this proton might be the plausible explanations, the rigid packing of the ribityl chain within the protein environment makes a change in the H^sC1' proton position very unlikely from a physical point of view. Therefore we considered the alternative possibility that the observed features actually consist of two superimposed signals: one corresponding to the H^sC1' hyperfine coupling that stays the same at both temperatures, and an additional signal at low temperatures that disappears in the 80 K spectrum.

Table 1.- Hyperfine constants obtained from pulsed-ENDOR measurements of WT-Fld and Lumi-Fld (Figures 2, 3 and 4). Some hyperfine constants and assignments come from previously reported results.

	Proton position	Signal label	Hyperfine principal constants (MHz)[a]
WT-Fld	H6	b	$A_1 = 4.3 \pm 0.5$, $A_2 = 5.5 \pm 0.2$, $A_3 = 6.1 \pm 0.2$
	$CH_3(8)$	c	$A_{\|\|} = 9.1 \pm 0.5$, $A_\perp = 8.0 \pm 0.1$
	H5[b]	f	$A_1 = -1.1 \pm 0.3$, $A_2 = -26.5 \pm 0,7$, $A_3 = -39.5 \pm 0.5$
	H^sC1'	d	$A_1 = 8.2 \pm 1.4$, $A_2 = 11.1 \pm 0.2$, $A_3 = 14.8 \pm 0.6$
	$CH_3(8)$	e	$A_{\|\|} = 17.5 \pm 1.0$, $A_\perp = 15.6 \pm 0.5$
Lumi-Fld	H6	b	$A_1 = 4.5 \pm 0.5$, $A_2 = 5.7 \pm 0.2$, $A_3 = 6.3 \pm 0.2$
	$CH_3(8)$	c	$A_{\|\|} = 9.7 \pm 0.4$, $A_\perp = 8.3 \pm 0.1$
	H5[b]	f	$A_1 = -0.8 \pm 0.5$, $A_2 = -26.5 \pm 0,7$, $A_3 = -39.5 \pm 0.7$
	$CH_3(10)$	d	$A_{\|\|} = 13.8 \pm 0.8$, $A_\perp = 11.6 \pm 0.3$
	$CH_3(8)$	e	$A_{\|\|} = 17.7 \pm 1.0$, $A_\perp = 15.7 \pm 0.5$
	$CH_3(10)$	g	$A_{iso} \approx 18.5$; $\Delta A \approx 9$

[a]The sign cannot be obtained from ENDOR measurements, it has been determined from DFT calculations[17,18] or HYSCORE experiments.[15,23]

[b]Data from HYSCORE experiments.[23]

Off-centered ENDOR spectra were recorded in order to check this alternative interpretation of our experiments. Due to the anisotropy of the N5, N10 and H5 hyperfine couplings, ENDOR measurements at the tail of the CW-EPR signal, that is, with the magnetic field shifted about 2 mT from the CW-EPR absorption maximum, result in some orientation selection. This means that such spectra are contributed mostly by molecules with the flavin ring nearly perpendicular to the direction of the magnetic field.[27,28] This orientation selection allows obtaining simpler features when the spectrum consists of many contributions from anisotropic hyperfine couplings. The orientation selected ENDOR spectra of WT-Fld taken at 15 K and 80 K are shown in Figure 2 (centre). As expected and previously reported for other flavoproteins,[27-29] features associated with H5, H6 and $CH_3(8)$ hyperfine couplings in the direction perpendicular to the flavin ring display a larger relative intensity. On the other hand, the spectrum at low temperature clearly displays two different and well separated signals in the (7 MHz-10 MHz) and (20 MHz-23 MHz) regions. One of them remains at 80 K while the other one (labelled as e in Figure 2) disappears. This last signal is located where the apparent

increase of the $H^{s}C1'$ hyperfine anisotropy is observed in the low temperature spectrum (Figure 2, top). This is a clear indication that the low temperature features in these regions actually correspond to two superimposed signals associated with the hyperfine couplings of different protons and hence they are labelled with with two different letters, d and e.

Provided that the signal d is associated to $H^{s}C1'$, the next question is to assign the additional signal e in the low temperature spectra. In an ENDOR study of another flavoprotein, Brosi et al.[30] reported temperature-dependent ENDOR features in these regions, assigning them to the hyperfine interaction with "arrested" (static) methyl protons at C8. To substantiate this assignment in our case, experiments were carried out using 8Cl-Fld, a sample where the protein was reconstituted with a FMN-analogue in which $CH_3(8)$ was changed to Chlorine.[22] Pulsed-ENDOR spectra of this sample at 15 K and 80 K (Figure 2, bottom spectra) show the same features as for WT-Fld, with two exceptions: signal c, assigned to $CH_3(8)$, and signal e are missing in the spectra of the analogue. This confirms the assignment of signal e to protons of the methyl group bound at C8.

To get further insight into the origin of the process taking place for $CH_3(8)$, we obtained the thermal evolution of the WT-Fld ENDOR spectrum. It should be taken into account that this process is potentially relevant for the better understanding of the FMN structure within the protein, as well as the electron transfer processes in which the flavin ring is involved. Figure 3 collects the pulse ENDOR spectra taken from 15 K to 80 K; the temperature evolution evidence that the height of signal e is reduced when temperature rises, disappearing above 45 K, while that of signal c increases from 35 K to 60 K and stays almost constant for higher temperatures.

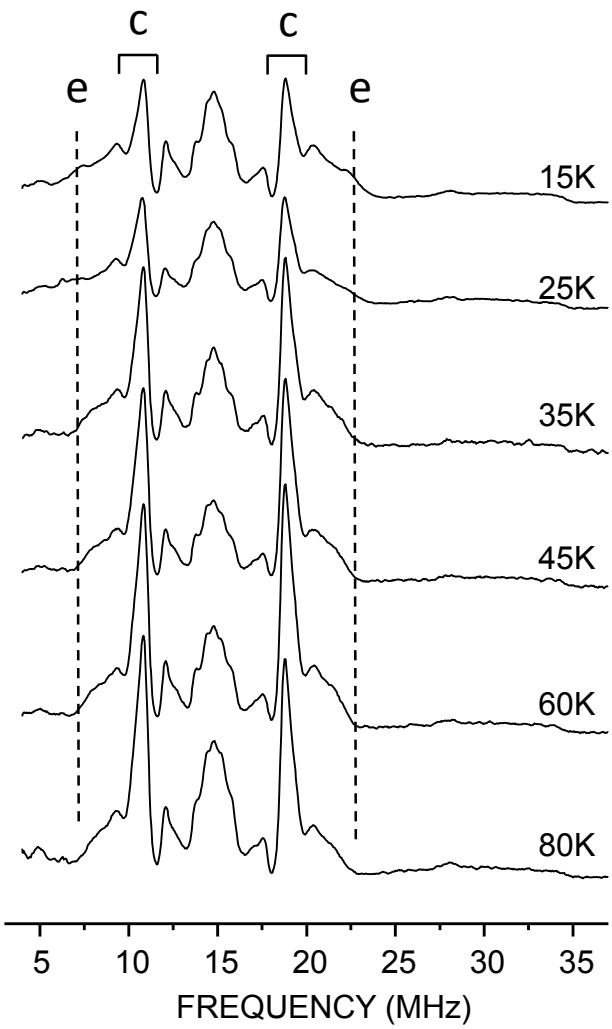

c.- $CH_3(8)^A$; e.- $CH_3(8)^{E+}$

Figure 3.- Thermal evolution of the pulsed-ENDOR spectrum of WT-Fld measured at the centre of the CW-EPR signal, from 15 K to 80 K. Signals c and e change with temperature: the first one gains intensity from 35 K to 60 K, and the second one decreases on going from 15 K to 35 K, disappearing above 45 K.

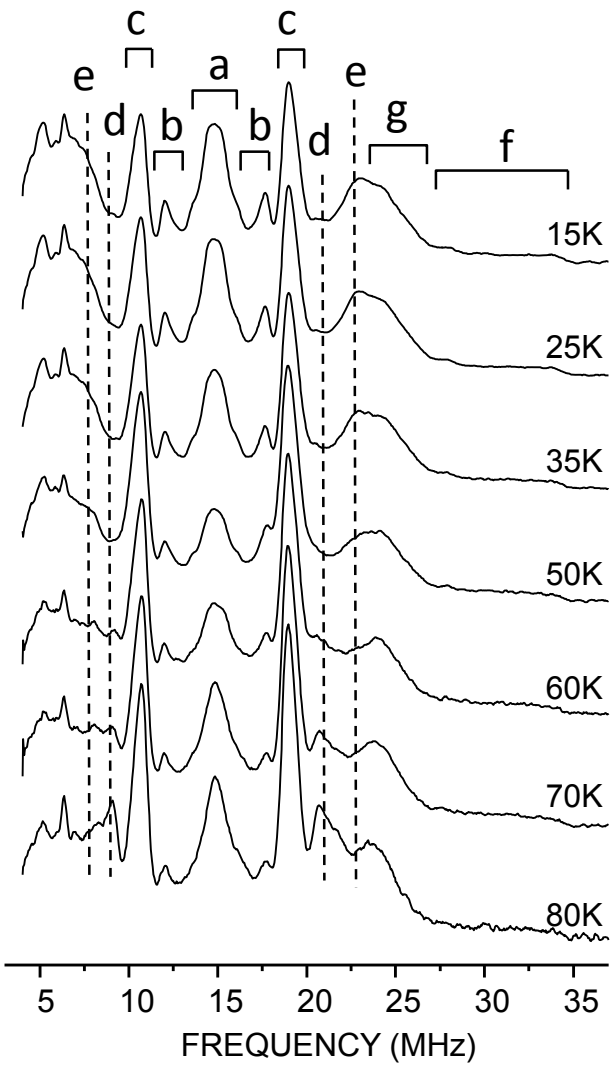

a.- "Matrix" protons; b.- H6; c.- $CH_3(8)^A$;
d.- $CH_3(10)^A$; e.- $CH_3(8)^{E+}$; f.- H5; g.-$CH_3(10)$

Figure 4.- Thermal evolution of the pulsed-ENDOR spectra of Lumi-Fld measured at the centre of the CW-EPR signal, from 15 K and 80 K. Spectral features are labelled in the same way as in Fig. 2. Assignments of signals a, b, c, e and f are the same, but signal d corresponds to the methyl group bound to N10, and signal g is assigned to protons of this methyl group as well (see text).

The thermal evolution of features c and e is depicted in Figure 5.A. Proper comparison of the signal heights requires careful rescaling of the spectra taken at different temperatures, which is not a trivial question, since several spectral features are superimposed, and underlying temperature-dependent signals can cause changes in the apparent intensity of features that could in principle be considered temperature-independent. The proton matrix line has been used in the past as a reference for quantification of intensity variations.[30] However, the numerous and unidentified contributions to this signal prevent guarantying temperature-independent line intensity. The same applies to signal b, assigned to H6, since it appears in a frequency region where other weakly coupled protons can contribute (hyperfine coupling constants around 4-6 MHz). On the other hand the feature corresponding to H5 interaction is properly isolated from any other contribution and is independent from temperature. For this reason, and in spite of the fact that this signal is weak, which could introduce some inaccuracy, we adopted H5 (signal f) as a reference for the intensity quantification shown in Figure 5.A. These results will be interpreted on the basis of a model of rotation for the methyl group that will be described below.

Since temperature-dependent couplings were observed also for Lumi-Fld,[16,23] the temperature evolution of ENDOR spectra was experimentally recorded for this sample in the same temperature range (15 K to 80 K), see Figure 4. Labels and assignments for the matrix protons (a), H6 (b) and H5 (f) are the same as in Figure 2 as the lines have the same shape and appear almost at the same positions (see Table 1). Also, the signals assigned to $CH_3(8)$ (c and e) are located at the same positions, and undergo a thermal process similar to the one detected in WT-Fld (see Figure 5.B).

The differences between the spectra of Lumi-Fld and WT-Fld arise in the signals from the substituent at N10 (C1' protons, labelled as d). For Lumi-Fld, there are three protons bound to C1', since a methyl group is bound to N10. CW-ENDOR spectrum of this sample at 120 K displayed features at about 9 and 11 MHz assigned to $CH_3(10)$ undergoing fast rotation.[16] The spectra here reported show that this signal (labelled as d in Figure 4) is not detected at low temperatures, appears above 60 K and shows a relatively important intensity only above 80 K. Additionally, another signal, labelled as g and assigned to $CH_3(10)$, is detected.

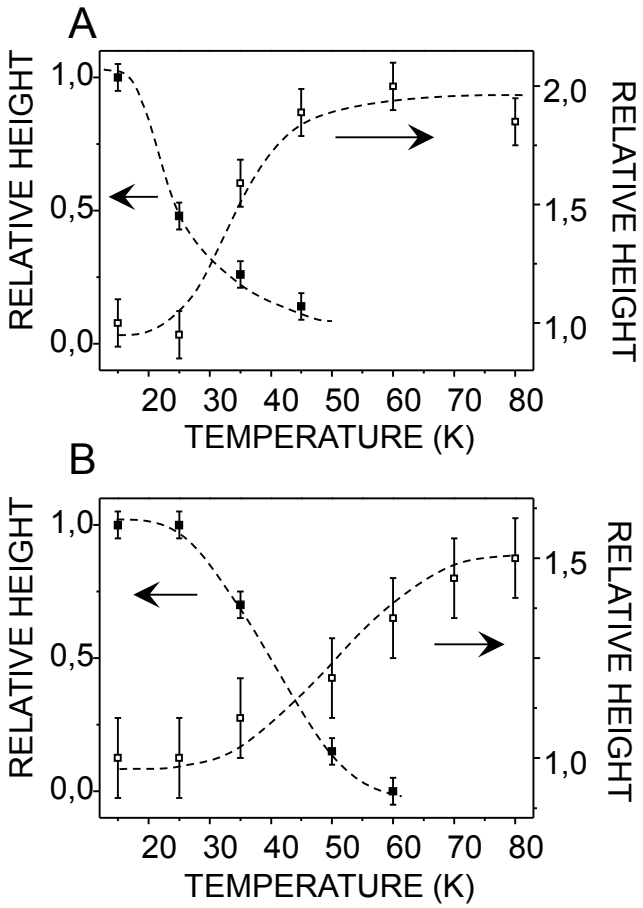

Figure 5: Plots for the thermal evolution of the heights of signals c (empty squares) and e (solid squares) assigned to $CH_3(8)$, in WT-Fld (A) and Lumi-Fld (B). The height of signal e was obtained by subtracting the high temperature ENDOR spectrum (60 K, that lacks signal e contributions) from the one at each temperature in such a way that the features d and g are eliminated. Heights are given relative to the ones at 15 K. Lines are just guides for the eye. The change in the activation temperature of the averaging process can be seen (see text).

2.2.- ANALYSIS OF THE RESULTS: METHYL ROTATION MODEL

When a methyl group is bound to an organic radical, the corresponding hyperfine couplings of its protons with the electronic spin can be detected in a magnetic resonance experiment. These couplings depend on both the position of the methyl protons with respect to the π semioccupied orbital and on the ability of the group to rotate around the carbon fourth bond axis. Taking the structure of the methyl group as static (rigid limit), the hyperfine interaction of every proton is contributed by an isotropic part that can be described with the hyperconjugation model:[31-33]

$$A_{iso}^{\ i} = b_o + b_2 \cos^2\phi_i \qquad i = 1 \text{ to } 3 \qquad [1]$$

Where i refers to each proton in the methyl group, and ϕ_i denotes the angle between the projection of the H_i-C bond onto the plane perpendicular to the fourth bond of the methyl carbon and the direction perpendicular to the flavin plane. Because of the methyl configuration, $\phi_3 = \phi_2 + 2\pi/3 = \phi_1 + 4\pi/3$. Usually $b_o << b_2$. Aditionally, hyperfine interactions also have anisotropic contributions, which are mainly due to dipolar interaction between the electronic and the nuclear spins. Therefore, in principle, for a methyl group in the rigid limit, one would expect three different proton couplings.

Beside this, the dynamics of the system, influencing the ENDOR spectrum of the methyl group coupled to the radical, must be also taken into account. Previous ENDOR studies on flavoproteins detected ENDOR features like signal c in Figure 2, and they usually interpreted them as due to a fast rotation averaging effect for the hyperfine coupling of $CH_3(8)$ of the flavin.[16] Our experiments indicate that at low temperature the signal c coexists with the signal e, also coming from the same methyl group. This behaviour is hard to be explained on the basis of previous interpretations because classical dynamical averaging should exclude the coexistence of static and averaged signals. Assuming that signal e comes from the hyperfine interaction with a proton of $CH_3(8)$ in the rigid limit, a classical dynamic process would predict that the signals coming from the static features would be the only ones seen at very low temperatures. As temperature increases, they should get broader (motional broadening regime), and finally merge into the fast rotating signal at higher temperatures (motional narrowing regime). Additionally, quantum rather than classical behaviour would be expected for the rotation of this methyl group at such low temperatures.

Analysis of the measured CH3(8) features requires a specific model. Rotation of the methyl group can be free or almost free, or can be hindered in some degree, from a weak to a very strong hindrance. In all cases, this rotation is typically a quantum motion, as the angular momentum of the methyl rotor is in the range of the Plank constant. A theoretical model for the analysis of the hyperfine coupling of protons from methyl groups in magnetic resonance spectra was first developed by Freed,[32] and further completed by Clough and others.[33-36] On the basis of this model, EPR and ENDOR spectra of organic radicals containing methyl rotors have been extensively described.[37-43] Those studies used the hyperfine splittings and the thermal evolution of the magnetic resonance signals to characterize the shape and depth of the rotational well that causes the hindrance of the methyl motion.

We will use the Freed-Clough model for the analysis of our results. To make this analysis easier to be followed, we will first present a brief summary of the model. Because of the quantized rotation modes of the methyl group, the corresponding magnetic resonance spectra, involving spin transitions, are no longer independent from the methyl group motion. The relevant quantum states for diagonallizing the spin Hamiltonian include electronic (orbital), rotational and spinorial parts, and have to fulfil the symmetry requirements of the system, namely C_3 point group symmetry and Pauli's principle.[32,33]

When rotation is weakly or not hindered, the methyl group reaches quantized rotational modes. On the other hand, for strong hindrance, motional modes are rather torsional oscillators within a rotational well $V(\phi)$ that can be described as

$$V(\phi) = (1/2)\, V_3\, [1- \cos 3(\phi-\phi_o)] \qquad [2]$$

Where ϕ is an angle that characterizes the methyl position and is defined in the same way as ϕ_i in Equation 1; ϕ_o is the angle for one the three minima of the rotational well and V_3 is the well depth.

For a classical rotor, this motion would be confined, with each proton just displaying a restricted rotational vibration around one of the well minima. However, due to the quantum character of the methyl rotor, a tunneling process takes places as far as the rotational well has a finite depth. The tunneling frequency (ω_t) corresponds to the energy splitting between the A singlet and the (E^A, E^B) doublet of the quasi degenerated

ground triplet of torsional states. This tunneling splitting and the depth of the rotational well are related in such a way that the larger the rotational well depth is, the smaller the tunneling frequency is. [32]

The actual signals observed in EPR or ENDOR spectra depend on the relative values of the tunneling and hyperfine energies. When the tunneling frequency is larger than the hyperfine splitting anisotropies, the proper functions describing the methyl states are symmetry-adapted combinations of the methyl protons placed in each of the three minima of the rotational well with the suited nuclear proton spin states.[32,33] As a consequence, ten allowed ENDOR transitions can be obtained. Their spectral positions at the first-order approximation are:

$$\begin{aligned} \omega^{A} &= \omega_{H} \pm (1/2)\, A_{iso}{}^{A} && \text{(multiplicity 3)} \\ \omega_{+}{}^{E} &= \omega_{H} \pm (1/2)\, (A_{iso}{}^{A} + A_{iso}{}^{E}) && \text{(multiplicity 1)} \\ \omega_{-}{}^{E} &= \omega_{H} \pm (1/2)\, (A_{iso}{}^{A} - A_{iso}{}^{E}) && \text{(multiplicity 1)} \end{aligned} \qquad [3]$$

where ω_H is the proton Larmor frequency, $A_{iso}{}^{A}$ is the average of the hyperfine isotropic constants of the protons at the three minima of the rotational well

$$A_{iso}{}^{A} = (A_{iso}{}^{1} + A_{iso}{}^{2} + A_{iso}{}^{3})/3 \qquad [4]$$

and $A_{iso}{}^{E} \approx 0{,}9\ A_{iso}{}^{A}$.[35] Second-order contributions depend on the hyperfine anisotropy and tunneling frequencies. For single crystal samples and well separated ENDOR spectral features, the observed second-order shifts allow estimating the tunneling frequency and consequently the rotational well depth.[33-35] It is worth noting that in the large tunneling frequency situation, the rigid-limit proton hyperfine splittings are never displayed in the ENDOR spectra, even at very low temperatures, and that together with the ω^{A} spectral features (placed in the position expected for a classical "fast rotation averaging"), the lines $\omega_{\pm}{}^{E}$ are detected as well. These features are not related with the rigid-limit splittings (for instance, their positions do not depend on the actual values of ϕ_o) and have no explanation from a classical point of view.

When tunneling frequency is smaller than hyperfine anisotropies, it can be considered as a perturbation of the rigid-limit hyperfine splittings and the ENDOR signals appear (first-order approximation) at frequencies:

$$\omega_i = \omega_H \pm (1/2)\, A^i \pm 2\omega_t/3 \qquad i = 1, 2, 3 \qquad [5]$$

where i accounts for each of the three methyl protons, A^i is the hyperfine constant, and ω_t is the tunneling frequency. Although in this case the spectra is more similar to the one expected for a classical rigid limit, the contribution of the tunneling frequency causes splittings and shifts of the signals that can be important.[36]

When temperature rises, the model predicts an evolution of the spectra. Classical thermal evolution would require a hopping process of the methyl group over the rotational well barrier. However, a different process at lower temperatures is able to cause averaging of the spectral features according to the quantum model. When the methyl state suffers a thermal promotion from any level of the ground triplet to one of the first excited triplet within the rotational well and goes back to any ground level, the jump does not preserve the wave function symmetry. This causes an averaging of the hyperfine anisotropy when the inverse of the correlation time of the process is larger than the anisotropy. It must be considered that the excited level can be also a torsional mode and have an energy quite lower that the classical barrier V_3. This process can be modelled as a simple Arrhenius thermal activation over a weaker "barrier" corresponding just to the energy of the first excited level. For large tunneling frequencies, this averaging process causes $\omega_{\pm}^{E}$ signals to broaden and collapse, and ω^{A} feature to grow. For small tunneling frequencies, rigid hyperfine features should disappear and averaged features at the corresponding ω^{A} positions should grow. Details of the thermal evolution depend on the actual dynamic process occurring in the given system. Nevertheless, again the averaging is predicted to occur at temperatures lower than the ones of a classical model.[33,44]

Positions of signals c and e together with their intensities as a function of temperature allow characterizing the behaviour of CH_3(8), both in WT-Fld (Figures 3 and 5.A) and Lumi-Fld (Figures 4 and 5.B). Results for both samples are similar. Position of signal e corresponds to a hyperfine constant about 1.9 times the one of signal c (cf. Equations 3 and 4). This, together with the fact that they are both detected at low temperatures, clearly indicate that those signals are related with ω^{A} and ω_{+}^{E} features in the large tunneling frequency limit for methyl rotation. ω_{-}^{E} signals are not resolved as they are expected to appear in the region of the matrix protons. The thermal evolutions

of these two features also follow the predictions of the model: ω_+^E lines start decreasing at a given temperature, and when temperature further rises ω^A features increase their intensity. All these changes take place in a rather narrow temperature region ($\Delta T \approx 30$ K) in both samples but, as mentioned previously, the activation temperature seems to be slightly higher for the Lumi-Fld sample.

Previous studies on methyl dynamics used the second order shifts in the position of the ENDOR lines to obtain the tunneling frequency.[33] Other methods were also based in the accurate estimation of the individual ENDOR features intensities.[41] Unfortunately, these strategies are unpractical in our system. It should be noted that most of the previous studies show methyl hyperfine splittings at least three times larger than the ones detected in our case, in such a way that they were resolved in the CW-EPR spectra, and each ENDOR signal could be obtained separately by exciting each CW-EPR line. In our case, we excite the unique CW-EPR signal and all the ENDOR features are simultaneously displayed in the spectra. As second order shifts are small, they are not expected to be resolved in our spectra. Additional difficulties for our analysis come from the fact that the methyl features are partially superimposed with those of the other protons in the ENDOR spectra, and all our evidences come from orientationally disordered samples. This makes it difficult to determine the positions and intensities of the individual lines with enough accuracy. At this stage, we only can infer that tunneling frequency is larger than the hyperfine anisotropy. Then $\omega_t \geq 10$ MHz and the well barrier[32] should have a higher limit $V_3/k \leq 1000$ K.

However, a previous study[45] pointed out that for many methyl rotors in different molecules a correlation exists between the tunneling frequency and the activation temperature of the averaging process. Assuming that this phenomenological relation also applies to methyl rotors bound to the flavin ring, we can estimate from the activation temperatures the three relevant parameters characterizing the rotational model for CH_3(8). The thermal evolution is activated at about 25 K for WT-Fld and at about 35 K for Lumi-Fld. From these values and following the correlations described in the work of Clough et al.[45] the tunneling frequency ω_t, the rotational barrier V_3, and the energy gap between the ground torsional state and the first excited torsional state E_{01} can be estimated. The results for WT-Fld and Lumi-Fld are collected in Table 2.

Table 2.- Parameters characterizing the rotational motion of methyl groups at positions C8 and N10 in WT-Fld and Lumi-Fld on the basis of the rotational hindrance well potential described in Equation 2. Values for CH_3(8) of WT-Fld (row 1) are used in Figure 6.

Sample	CH_3 position	T_{act} (K)[a]	ω_t (MHz)	V_3/k (K)	E_{01}/k (K)
WT-Fld	C8	≈ 25	280 ± 100	570 ± 30	180 ± 10
Lumi-Fld	C8	≈ 35	70 ± 50	750 ± 30	200 ± 10
Lumi-Fld	N10	≈ 55	2 ± 1	≈ 1500	≈ 280

[a]Activation temperature for the averaging of the ENDOR features

Although the behaviour of the methyl bound to N10 in Lumi-FLld is less relevant from a functional point of view, we can also obtain some ideas about its rotation. Several details of the measured spectral features are important for this description:

-The averaged ω^A feature (signal d) is not seen at low temperatures, indicating that the system dynamics corresponds to the small tunneling frequency limit.

-At low temperatures one very intense feature (g) related with these methyl protons is resolved.

-The rigid hyperfine splittings calculated for these protons[17,18] indicated that the hyperfine anisotropy is $\Delta A_i = |(A_i)_{\|} - (A_i)_{\perp}| < 4{,}5$ MHz. However, the anisotropy associated to the signal g is $\Delta A_g \approx 9$ MHz.

For a static methyl group, the hyperfine splitting of each proton can be related with their orientation using Equation 1. Because of the methyl symmetry, the averaged methyl hyperfine constant A_{iso}^A can be obtained as a function of b_o and b_2 (cf. Equations 1 and 4)

$$A_{iso}^A = b_o + 0{,}5\, b_2 \qquad [6]$$

Then we can estimate $b_2 \approx 25$ MHz from the position of signal d in Figure 4, and ϕ from signal g, $\phi_g \approx 30^o$. As the three ϕ_i angles of the methyl protons differ by 120º, this result indicates that one of the methyl protons lies in the plane of the flavin ring, displaying almost no hyperfine splitting, while the two others are magnetically equivalent, $\phi \approx 30^o$.

Then, signal g consists of the superposition of their two features. This would explain the relatively large intensity of this signal.

So far we have ignored the contribution of the tunneling frequency. Its first-order effect is to split the ENDOR lines symmetrically with respect to the static line (see Equation 5). If the contribution is small enough to keep the two signals unresolved, the aspect of the spectral feature would be a single line centred at the static hyperfine splitting, but showing an apparently larger anisotropy, just like the one detected in Lumi-Fld. This allows estimating the tunneling splitting $\omega_t \approx$ 1-2 MHz. A smaller ω_t would not account for the apparent anisotropy of the signal g, and a larger one would cause signal g to be split in at least two. From this estimation of ω_t, V_3 and E_{01} for the methyl group bound to N10 in Lumi-Fld sample are subsequently estimated (Table 2).

The obtained values can be used for predicting the temperature for the activation of the averaging of CH_3(10). Following Clough et al.[45] this temperature would be 55 K, in fair agreement with our experimental results (ω^A of this methyl group grows between 60 K and 80 K, see Figure 4).

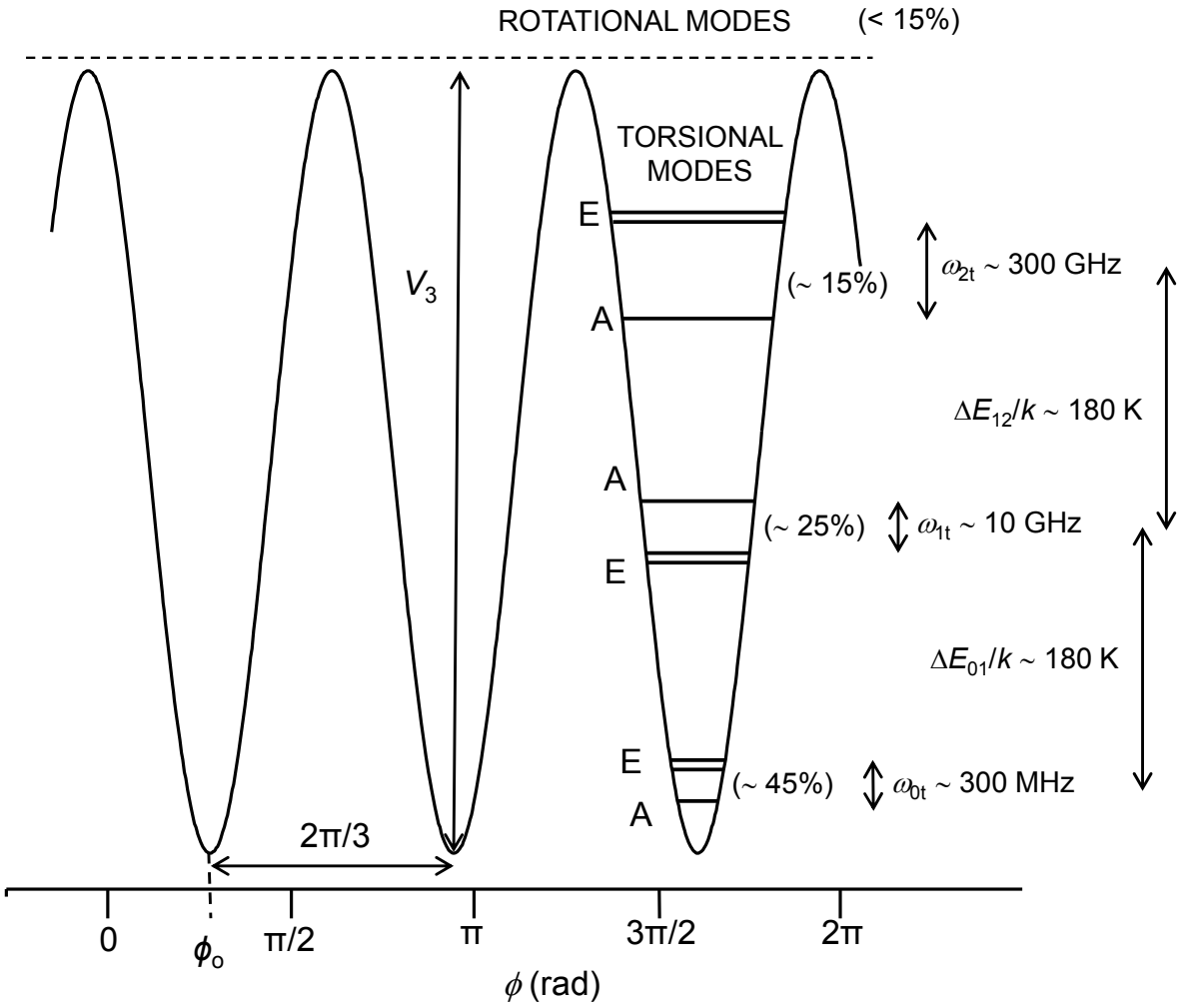

Figure 6.- Scheme of the relevant rotational-torsional states for $CH_3(8)$ in the flavin of WT-Fld. V_3 and ϕ_o account for the depth and equilibrium position of the torsional well, respectively. Three torsional modes (with energies below V_3, the well maximum) are accessible for the system. They consist in triplets of quasi degenerated energy levels, split in a singlet A and a doublet (E^A, E^B). The tunneling frequencies ω_{it} are indicated for each torsional mode. The energy gap of the modes is indicated, and the percent numbers in brakets correspond to the thermal population of the mode at room temperature. The scale of the tunneling splitting has been exaggerated in the picture to make it clearer. Note that although the energy of the torsional modes is drawn in one of the rotational well lobes, they actually consist in resonant functions of the methyl protons at the three lobes simultaneously. Rotational modes are over the well maximum, and are sparsely populated.

2.3.- A MODEL FOR THE ROTATIONAL STATES OF THE METHYL GROUPS OF THE FLAVIN RING AT ROOM TEMPERATURE

The results obtained from ENDOR measurements at low temperatures display a picture for the rotational state of the methyl group of the flavin quite different from the one conventionally used. Rather than as fast rotating methyl groups, they behave as rotors locked by a large barrier that simoultaneously show specific quantum properties. A picture for the energies of rotational states of $CH_3(8)$ in WT-Fld is depicted in Figure 6. Its main characteristics are the following:

-Free rotational modes ($E > V_3$) are sparsely populated even at room temperature.

-Tunneling motion through the rotational barriers is allowed because of the quantum nature of the methyl rotor. The frequencies for this motion correspond to ω_{it}, being in the range of microwave frequencies.

-At biologically relevant temperatures (~ 300 K), dynamic phenomena cause both decorrelation of the methyl tunneling states and changes in the rotational well shape, in such a way that a classical jump model would be able to describe the experimental evidence from EPR or ENDOR. However, at these temperatures about a half of the methyl groups are in the ground triplet, while most of the rest occupy excited torsional oscillator modes within the potential well. For all of them, angular positions of the methyl protons are restricted to a rather narrow angle around the equilibrium angles. Changes in the states by hopping just rotate the methyl group a fixed angle ($\Delta\phi \approx 0$, $2\pi/3$ or $4\pi/3$) and can be considered slow in comparison to electronic processes.

Details of this model depend on the actual shape and depth of the rotational barrier, but large hindrance of $CH_3(8)$ rotation might be a general property in flavoproteins. In fact, ENDOR features compatible with this model have been already reported, although at that point they were not related with tunneling effects.[30,46]

Interactions within the flavin ring (steric, electrostatic) will contribute to the rotational hindrance. In this sense, it must be taken into account that the closest substituents of the flavin to $CH_3(8)$ are $CH_3(7)$ and H9. The minimum distance between a proton of $CH_3(8)$ and these other protons is about 2,4 Å, and even a coupling between $CH_3(8)$ and $CH_3(7)$ rotors cannot be excluded. Other interactions external to the flavin ring (interactions with the apoprotein pocket, protein partners or substrates), as well as diffuse environment conditions (such as electric polarizability or pH) are also expected to cause a large influence on the rotation hindrance. In this sense, interesting results

previously reported in a different flavoprotein[30] describe the influence of the nearest residues on the methyl rotation hindrance. The analysis of those results should perhaps be revised, as the contribution of the quantum tunneling on the ENDOR spectra was not considered. However, the activation temperatures obtained for the changes in the ENDOR features can be interpreted on the basis of the model described here since rotation barriers seemed to be of the same order as the ones obtained in our study (between 500 K and 1500 K).

Besides the rotation barrier depth, another important parameter is the position of the equilibrium angles (ϕ_o in Figure 6). Again intramolecular, flavin-apoprotein and flavin-substrate interactions can affect the actual value of ϕ_o in a given flavoprotein. As methyl protons are mainly oriented at the ϕ angle minima, this also determines the electronic orbital in the flavin semiquinone state. The symmetry-adapted contribution of the 1s orbital from the methyl protons to the SOMO is:[31,32]

$$\psi_o^{elec} = N^{1/2} [\cos \phi \, \Phi_{H1}{}^{1s} + \cos (\phi + 2\pi/3) \, \Phi_{H2}{}^{1s} + \cos (\phi + 4\pi/3) \, \Phi_{H3}{}^{1s}] \qquad [7]$$

where N is a normalization constant. As the methyl orientation is restricted by the rotational well, the actual contribution corresponds to $\phi \approx \phi_o$. This should have also an effect in the mechanism of electron transfer. For instance, the methyl orientation will play a relevant role to form short-living reaction intermediates or tunneling paths for electron transfer, and a methyl group with a rather restricted orientation seems more appropriated than a fast rotating one to achieve the chemical process. Indeed, this provides the protein with a simple mode for controlling the flavin reactivity just by modulating the orientation minima of $CH_3(8)$ rotation. In this sense, it is worth noting that previous studies[25,30] indicated a correlation between rotational hindrance and chemical relevant properties, as photochemical activity in phototropins or pH dependent reactivity in (6-4) photolyases, while others suggested that position 8 of the flavin modulates the electronic and oxido-reduction properties of Fld.[6,22]

3.- CONCLUSIONS

The results of our study demonstrate that the methyl group bound at position 8 of the flavin ring behaves as a quantum rotor locked by a rather high barrier ($V_3/k \geq 500$ K). The analogous $CH_3(7)$ group is likely to behave similarly. At low temperatures

methyl dynamics are driven by tunneling transitions between the three equilibrium positions. Interestingly, at room temperature methyl rotors are still locked and reorientation of the methyl group takes place by means of a hopping process.

Many studies had emphasized some physicochemical properties (redox states, electronic structure…) of the flavin ring in connection with the function of flavoproteins as they can be controlled by the interactions between flavin and its environment (apoprotein, substrate…). In this sense, it is worth noting that flavin methyl groups have also unique properties because of the quantum character of their reorientation dynamics. They are usually placed close to the substrate in ET processes and interactions with the apoprotein can also control the rotation barrier. All these features point to a relevant role of the methyl orientation and dynamics in the reactivity of flavoproteins that should be further investigated.

4.- EXPERIMENTAL SECTION

Sample preparation

Anabaena WT-Fld, Lumi-Fld and apoflavodoxin reconstituted with the 8-nor-Cl-FMN analogue (with the methyl bound to C8 replaced by chlorine, hereafter 8Cl-Fld) were prepared as indicated elsewhere and equilibrated in 10 mM HEPES, pH 7.0.[15,16,22] Samples with a protein concentration of 400–800 μM were placed in 3 mm EPR tubes and anaerobically reduced under an argon atmosfere to the neutral semiquinone state by either light irradiation with a 250 W slide projector, at 4 ºC in the presence of 20 mM EDTA and 2.5 μM 5-deazariboflavin, or, in the case of 8Cl-Fld, by stepwise dithionite addition.

Samples were then frozen and stored in liquid nitrogen (at 77 K) until used for the measurements.

Pulse ENDOR measurements

X-band pulse ENDOR experiments involving microwave (mw) and radio frequency (rf) pulses were performed in an Elexsys E-680 spectrometer from Bruker BioSpin Inc. The resonator, also from Bruker, was an ER MD4-EN dielectric ring of about 9.77 GHz resonance frequency equipped with an ENDOR coil. The temperature in the sample space was regulated using a continuous gas-flow cryostat and a temperature controller, both from Oxford Instruments Inc.

The measurements were performed using the Davies ENDOR experiment,[24] with pulse sequence $(\pi)_{mw} - T_1 - (\pi)_{rf} - (\pi/2)_{mw} - \tau - (\pi)_{mw} - \tau$ – echo and mw pulse lengths $t_{\pi/2}$ = 100 ns and t_{π} = 200 ns. The interpulse delays were T_1 = 17 μs and τ = 208 ns. A rf π pulse of length 15 μs was applied during T_1 and its frequency was varied between 4 and 40 MHz. The entire pulse sequence was repeated with a frequency of 200 Hz at 80 K; at lower temperatures, the repetition frequency had to be decreased due to slower relaxation of the electron spin and at 15 K was only 33 Hz.

ACKNOWLEDGMENTS

This work was supported by the Spanish Ministry of Economy and Competitivity (MINECO), Grants No. MAT2011-23861 to JIM, and BIO2010-14983 14983 and BIO2013-42978-P to MM, and by the program ‘‘Grupos de investigación’’ of the Autonomous Government of Aragón, Refs. B18 and E33.

REFERENCES

[1] *Chemistry and Biochemistry of Flavoenzymes*, ed. F. Müller, CRC Press, Boca Raton, FL, 1990.

[2] P. Macheroux, B. Kappes and S. E. Ealick, *FEBS J.*, 2011, **278**, 2625-2634, and references therein.

[3] S. G. Mayhew, G. P. Foust and V. Massey, *J. Biol. Chem.*, 1969, **244**, 803–810.

[4] A. K. Arakaki, E. A. Ceccarelli and N. Carrillo, *FASEB J.*, 1997, **11**, 133–140.

[5] M. L. Ludwig, K. A. Pattridge, A. L. Metzger, M. M. Dixon, M. Eren, Y. Feng and R. P. Swenson, *Biochemistry*, 1997, **36**, 1259–1280.

[6] I. Lans, S. Frago and M. Medina, *Biochim. Biophys. Acta*, 2012, **1817**, 2118–2127.

[7] D. C. Haines, I. F. Sevrioukova and J.A. Peterson, *Biochemistry*, 2000, **39**, 9419–9429.

[8] L. H. Bradley and R.P. Swenson, *Biochemistry*, 2001, **40**, 8686–8695.

[9] F. Chang, L. H. Bradley and R. P. Swenson, *Biochim. Biophys. Acta*, 2001, **1504**, 319–328.

[10] A. A. McCarthy, M. A. Walsh, C. S. Verma, D. P. O'Connell, M. Reinhold, G. N. Yalloway, D. D'Arcy, T. M. Higgins, G. Voordouw and S. G. Mayhew, *Biochemistry*, 2002, **41**, 10950–10962.

[11] I. Nogués, J. Tejero, J. K. Hurley, D. Paladini, S. Frago, G. Tollin, S. G. Mayhew, C. Gómez-Moreno, E. A. Ceccarelli, N. Carrillo and M. Medina, *Biochemistry*, 2004, **43**, 6127-6137.

[12] T. Iyanagi, *Biochem. Biophys. Res. Commun.*, 2005, **338**, 520–528.

[13] I. Lans, M. Medina, E. Rosta, G. Hummer, M. Garcia-Viloca, J. M. Lluch and À. González-Lafont, *J. Am. Chem. Soc.*, 2012, **134**, 20544-20553.

[14] J. R. Peregrina, I. Lans and M. Medina, *Eur Biophys J.*, 2012, **41**, 117-128.

[15] J. I. Martínez, P. J. Alonso, C. Gómez-Moreno and M. Medina, *Biochemistry*, 1997, **36**, 15526-15537,

[16] M. Medina, A. Lostao, J. Sancho, C. Gómez-Moreno, R. Cammack, P. J. Alonso and J. I. Martínez, *Biophys. J.*, 1999, **77**, 1712-1720.

[17] S. Weber, K. Möbius, G. Richter and C. W. M. Kay, *J. Am. Chem. Soc.*, 2001, **123**, 3790-3798.

[18] J. I. García, M. Medina, J. Sancho, P. J. Alonso, C. Gómez-Moreno, J. A. Mayoral and J .I. Martínez, *J. Phys. Chem. A*, 2002, **106**, 4729-4735.

[19] I. Nogués, L. A. Campos, J. Sancho, C. Gomez-Moreno, S. G. Mayhew and M. Medina, *Biochemistry*, 2004, **43**, 15111–15121.

[20] S. Frago, G. Goñi, B. Herguedas, J. R. Peregrina, A. Serrano, I. Pérez-Dorado, R. Molina, C. Gómez-Moreno, J. A. Hermoso, M. Martínez-Júlvez, S. G. Mayhew and M. Medina, *Arch. Biochem. Biophys.*, 2007, **467**, 206–217.

[21] G. Goñi, B. Herguedas, M. Hervás, J. R. Peregrina, M. A. De la Rosa, C. Gómez-Moreno, J. A. Navarro, J. A. Hermoso, M. Martínez-Júlvez and M. Medina, *Biochim. Biophys. Acta*, 2009, **1787**, 144–154.

[22] S. Frago, I. Lans, J. A. Navarro, M. Hervás, D. E. Edmondson, M. A. De la Rosa, C. Gómez-Moreno, S. G. Mayhew and M. Medina, *Biochim. Biophys. Acta*, 2010, **1797**, 262-271.

[23] J. I. Martínez, P. J. Alonso and M. Medina, *J. Mag. Reson.*, 2012, **218**, 153-162.

[24] A. Schweiger and G. Jeschke, *Principles of pulse electron paramagnetic resonance*, Oxford University Press, Oxford, 2001, pp 359 ff.

[25] E. Schleicher, R. Bittl and S. Weber, *FEBS J.*, 2009, **276**, 4290-4303.

[26] E. Schleicher and S. Weber, *Top.Curr. Chem.*, 2012, **321**, 41-66.

[27] L. E. G. Eriksson and A. Ehrenberg, *Biochim. Biophys. Acta*, 1973, **293**, 57-66.

[28] P. Macheroux, J. Petersen, S. Bornemann, D. J. Lowe and R. N. F. Thorneley, *Biochemistry*, 1996, **35**, 1643-1652.

[29] S. Weber, C. W. M. Kay, A. Bacher, G. Richter and R. Bittl, *ChemPhysChem*, 2005, **6**, 292-299.

[30] R. Brosi, B. Illarionov, T. Mathes, M. Fisher, M. Joshi, A. Bacher, P. Hegemann, R. Bittl, S. Weber and E. Schleicher, *J. Am. Chem. Soc.*, 2010, **132**, 8935-8944.

[31] R. Bershon, *J. Chem. Phys.*, 1956, **24**, 1066-1070.

[32] J. H. Freed, *J. Chem. Phys.*, 1965, **43**, 1710-1720.

[33] S. Clough and F. Poldy, *J. Chem. Phys.*, 1969, **51**, 2076-2084.

[34] S. Clough, J. Hill and F. Poldy, *J. Phys. C: Solid State Phys.*, 1972, **5**, 518-528.

[35] S. Clough and F. Poldy, *J. Phys. C: Solid State Phys.*, 1973, **6**, 1953-1964.

[36] S. Clough, J. R. Hill and M. Punkkinen, *J. Phys. C: Solid State Phys.*, 1974, **7**, 3779-3784.

[37] L. D. Kispert, T. C. S. Chen, J. R. Hill and S. Clough, *J. Chem. Phys.*, 1978, **69**, 1876-1880.

[38] W. Unruh, T. Gedayloo and J. D. Zimbrick, *J. Phys. Chem.*, 1978, **82**, 2016-2022.

[39] K. Toriyama, M. Iwasaki, K. Nunome and H. Muto, *J. Chem. Phys.*, 1981, **75**, 1633-1638.

[40] K. Matsuki and I. Miyagawa, *J. Chem. Phys.*, 1982, **76**, 3945-3952.

[41] M. Brustolon, T. Cassol, L. Micheletti and U. Segre, *Mol. Phys.*, 1986, **57**, 1005-1014.

[42] F. Bonon, M. Brustolon, A. L. Maniero and U. Segre, *Chem. Phys.*, 1992, **161**, 257-263.

[43] A. Krivokapić, K. T. Øhman, W. H. Nelson, E. O. Hole and E. Sagstuen, *J. Phys. Chem. A*, 2009, **113**, 9633-9640.

[44] J. L. Carolan, S. Clough, N. D. McMillan and B. Mulady, *J. Phys. C: Solid State Phys.*, 1972, **5**, 631-640.

[45] S. Clough, A. Heidemann, A. J. Horsewill, J. D. Lewis and M. N. J. Paley, *J. Phys. C: Solid State Phys.*, 1981, **14**, L525-L529.

[46] B. Barquera, J. E. Morgan, D. Lukoyanov, C. P. Scholes, R. B. Gennis and M. J. Nilges, *J. Am. Chem. Soc.*, 2003, **125**, 265-275.